Orbiter Rarefied-Flow Reentry Measurements from the OARE on STS-62

Robert C. Blanchard
NASA Langley Research Center
Hampton, Virginia 23681-0001

John Y. Nicholson
ViGYAN, Inc.
Hampton, Virginia 23666-1325

Abstract

Acceleration data taken from the Orbital Acceleration Research Experiment (OARE) during reentry on STS-62 has been analyzed using calibration factors taken on-orbit. The data examined include the flight regime from orbital altitudes down to about 100 km which covers the free-molecule-flow regime and the upper altitude fringes of the flow-transition into the hypersonic continuum. Ancillary data on Orbiter position, orientation, velocity, and rotation rates have been used in models to transform the measured accelerations to the Orbiter center-of-gravity, from which aerodynamic accelerations along the Orbiter body axes have been calculated. Additional steps are discussed which remove residual offsets introduced in the measurements by Orbiter forces which are not modeled. The resulting aerodynamic accelerations, and in particular, the normal to axial acceleration ratio are discussed and compared with free-molecule-flow predictions of the normal to axial force aerodynamic coefficient ratios.

Nomenclature

A	acceleration component
C_A	axial coefficient
C_N	normal coefficient
C_Y	side force coefficient
g	gravitational acceleration (9.80665 m/s^2)
micro-g	μg
nano-g	ng

p,q,r	body rotation rates
V_a	air relative velocity
X, Y, Z	sensor or body axes
α	angle of attack
β	side-slip angle
ng	1×10^{-9} g
μg	1×10^{-6} g

subscripts

b	body axes
x,y,z	coordinate axes

Acronyms

APU	Auxiliary Power Unit
FES	Flash Evaporator System
GSE	Ground Support Equipment
HiRAP	High Resolution Accelerometer Package
JSC	Johnson Space Center
MSID	Measurement / Stimuli Identification
MET	Mission Elapsed Time
OARE	Orbital Acceleration Research Experiment
OMS	Orbiter Maneuvering System
STS	Shuttle Transportation System

Introduction

The Orbital Acceleration Research Experiment[1] (OARE) contains a tri-axial accelerometer which uses a single free-floating (non-pendulous) electrostatically suspended cylindrical proof-mass. The accelerometer sensor assembly is mounted to a microprocessor-controlled, dual-gimbal platform in order to perform in-flight calibrations. OARE 's objective is to measure Orbiter aerodynamic performance on orbit and during the initial stages of reentry. Thus, the OARE instrument is purposely designed for low-frequency signals only. As the low-frequency acceleration environment contains a variety of components (e.g. gravity-gradient, rotational effects), models of these components embedded in the acceleration measurements are required in order to extract the Orbiter aerodynamic acceleration signal. These models require additional measurements (e.g. vehicle position, velocity, orientation and angular rates) which are obtained by the Shuttle Project Office as standard ancillary data on any Orbiter mission. The models and measurements required to separate the components of low-frequency acceleration are discussed in the appendix of reference 2.

This report presents the data analysis used to extract the aerodynamic signals from the OARE measurements taken during reentry on the STS-62

mission. This is the first Orbiter mission which collected valid OARE data during the Orbiter reentry phase.

Instrument Synopsis

A brief overview of the instrument system is given for completeness. More details are given in reference 1. A schematic of OARE showing the various instrument components is shown on Figure 1. The instrument system weighs 53.2 kg (117 lbs.) and requires 110 watts of power. The OARE system consists of three line replaceable units which are mounted to a keel bridge mounting plate. The three units are: (1) the calibration table and sensor package, (2) the interface electronics, power system and servo control modules, and (3) the 16-bit programmable micro-computer and memory. The complete system dimensions are 43.2 x 33 x 104.1 cm (17 x 13 x 41 in.). The OARE is mounted on a keel bridge of the Orbiter at bay 11 on the cargo bay floor, as shown schematically on Fig. 2. The OARE sensor axes are co-aligned with the Orbiter body axes as shown on this figure. The relationship between the OARE coordinates system and the body axes coordinate system is:

$$\begin{pmatrix} X \\ Y \\ Z \end{pmatrix} = \begin{pmatrix} 1 & 0 & 0 \\ 0 & 1 & 0 \\ 0 & 0 & 1 \end{pmatrix} \begin{pmatrix} X_b \\ -Z_b \\ Y_b \end{pmatrix} \quad .$$

The accelerometer sensor (labeled "sensor package" in Figs. 1) is attached to a moveable platform. The platform is moveable about two axes, the inner-gimbal and the outer-gimbal axis, by two brushless DC torque motors, as illustrated in Fig. 1. There are 3 sensor ranges, A, B, and C, which correspond to acceleration scales of $\pm$10,000, $\pm$1000 and $\pm$100 μg respectively for the X-axis and $\pm$25,000, $\pm$1970 and $\pm$150 μg respectively for the Y- and Z-axes. The best sensor resolution is 3.05 x 10^{-9} g which is along the X-axis. The Y- and Z- axes have a slightly larger sensor resolution value of 4.6 x 10^{-9} g.

Trajectory Information

For each Orbiter mission, the Orbiter Project Office at JSC provides trajectory data. These data are available prior to the flight and are subsequently updated after the flight using measurements taken during the mission. These data provide the "as flown" information required by payload experiments for any particular mission.

Fig. 3 shows the altitude and air relative velocity, V_a of the STS-62 mission as a function of MET for the initial portion of the reentry on the STS-62 flight. The data shown relate to the OARE measurement period and, thus, cover a time period which corresponds to about 1 hour prior to deorbit burn when the OARE reentry flag was initiated from the ground flight-controllers to about 90 km in altitude after which the OARE sensors become saturated. The deorbit burn, at about 334.4 h MET, is clearly evident in Fig. 3. After the deorbit

maneuver the Orbiter is placed on a conic with a lower periapsis which accounts for the subsequent increase in velocity as the Orbiter approaches its new periapsis. Further down the velocity curve, the more dense atmosphere is encountered which provides another dramatic change in velocity as the Orbiter departs from its conic behavior due to increasing atmospheric effects.

The Orbiter attitude is changing during this time period shown on Fig. 3. Fig. 4 shows the orientation of the Orbiter in terms of the wind angles, namely, angle-of-attack, α and side-slip angle, β. These angles have been calculated from the body quaterion and velocity data sets used by the Orbiter navigation system provided by JSC. Clearly seen on the figure are large changes in α prior to and after deorbit burn. Prior to deorbit burn, the spacecraft is maneuvering using its primary and verniers thrustors to place the tail of the vehicle into the direction of motion in order to effect a change in orbit by the OMS rocket motors. After the orbit burn, the Orbiter performs a large positive pitch maneuver to orient the spacecraft into its preferred entry attitude of 40 deg. These motions induce acceleration inputs into the OARE which must be accounted for in order to extract the aerodynamic signal. Also, the rapid change in environment (due to orientation changes) provides a challenge to acquire reliable calibration data.

Aerodynamic Information

Based upon the preceding wind angle information for the STS-62 mission, it is possible to provide the predicted aerodynamics. Fig. 5 shows the three body axes aerodynamic coefficients, C_A, C_Y, C_N for the entire reentry period under investigation. These data are from the Orbiter Project Office[3] for the condition when Orbiter payload doors are closed. The aerodynamic data are from free-molecule-flow calculations generated by dividing the Orbiter surface geometry into multiple flat-plates and assuming fully diffuse surface reflection conditions. There are several points to be made from these graphs. First, the curves are not applicable for all the time when α is equal to 40 deg. (where the values are near constant) since this is the region when the vehicle begins to transition from the free-molecule flow to the hypersonic continuum. Second, there are instances during flight when a given Orbiter body axis is perpendicular to the flow thus providing zero values for its coefficient. This will provide extremely valuable offset checks in the analysis discussed later.

Data Processing

Initial Processing

Reentry data from OARE is not processed *in situ* by the OARE computer during the flight. This is in contrast to the OARE data taken in orbit which is processed on-board in order to compress the information to conserve computer memory space during flight. After the mission, the OARE reentry file is downloaded from the OARE memory in a raw digital format which provides the OARE measurements in a coded bit structure. This raw flight data file is

processed first in order to transform the flight data into useful quantities such as the accelerations (in counts) along the X-, Y-, and Z-axes along with numerous other information such as MET time, gimbal angles, the range code of each axis, bias and scale factor calibration flags, various temperatures, etc. The details of the raw digital format are given in reference 4.

The acceleration data rate is 10 samples/second. The three accelerations measurements are first changed to engineering units from counts assuming bias = 0 and the scale-factor ratio = 1. The transformation, which is axis and range dependent, is as follows:

$$A(x_i, r_j) = \frac{20\left[32768 - K(x_i, r_j)\right]}{65536} F(x_i, r_j) \quad , \mu g \qquad ,$$

where x_i= X, Y, or Z axis, and r_i= A, B, or C range, and where $K(x_i,r_i)$ are the corresponding measured counts, and $F(x_i,r_i)$ is given in the following Table 1:

Table 1 Values of function, $F(x_i,r_i)$

AXIS		RANGE	
	A	B	C
X	1000	100	10
Y	2500	197	15
Z	2500	197	15

Calibration Factors

Bias and scale-factor ratio measurements are used to produce the best estimates of the X, Y, and Z-axis absolute accelerations at the OARE sensor location. Bias and scale factor measurements are made by the OARE throughout the entire mission. The entire mission calibration data set provides insights into the validity of the calibration process. This procedure also provides estimates of the errors associated with generating absolute accelerations which are necessary for producing reliable aerodynamic accelerations, particularly at the micro-g level. The details on how these measurements are made and interpreted have been described in the literature[5] and will not be repeated here.

The bias and scale factor data throughout the entire STS-62 mission have been carefully examined and the results reported in reference 5. This ensemble of flight data has been used to obtain the values applicable for the reentry phase. The calibration values used in the analysis in this report are given in Table 2.

Table 2. STS-62 Reentry Calibration Factors

RANGE	AXIS	Bias, ug
A	X	-6.638
A	Y	+1.144
A	Z	-136.566
B	X	-.099
B	Y	+.721
B	Z	-14.158
C	X	+.048
C	Y	+.737
C	Z	-7.288

RANGE	AXIS	Scale Factor
A	X	1.03
A	Y	1.12
A	Z	1.09
B	X	1.02
B	Y	1.13
B	Z	1.11
C	X	1.01
C	Y	1.14
C	Z	1.08

The biases and scale factor measurements taken after the reentry mode was initiated are unreliable due to the active spacecraft maneuvering (which provides a rapidly changing environment), extraneous noise, and large frequency of thrustor firings. Meaningful biases are determined using the data just prior to the reentry mode initiation, between approximately 0.6 and 20.4 hours prior to deorbit burn initiation. During this interval 6 data points are examined, but only two are reliable due to the maneuvering being done by the Orbiter to orient itself in preparation for deorbit. The bias value results are given in Table 2.

The scale factors tend to remain constant throughout the flight. The scale factors were divided into four categories; (1) high rate, normal direction,

(2) high rate, reverse direction, (3) low rate, normal direction, and (4) low rate, reverse direction. High and low excursions are eliminated from each calibration data set and then the averaged scale factor is calculated from each set. Then, the average of all four sets is found and is given in Table 2, except the C-range, Z-axis values.

The scale factors for the C range, Z -axis are found to be unreliable for all OARE flights to date. To circumvent this problem, the scale factor calibration deduced from the Orbiter rotation about the center-of-gravity have been used. In effect, on any axis and in any sensor range the OARE scale factor calibration is accomplished by rotating the sensor on its platform to generate a known g-field from which the sensor output is scaled (the mechanism is like operating a precision centrifuge). An equivalent scale factor effect can be generated by holding the sensor motionless and rotating the spacecraft. This has been accomplished successfully on past Orbiter missions and Orbiter maneuvers compare well with scale factor results generated from the OARE calibration station, when reliable data is obtained[2]. Thus, there is reason to believe that the Z-axis scale factor determined by the flight maneuver is applicable since the maneuver data closely match the other two axes. Thus, the scale factor used in this analysis was the value determined during maneuvers on STS-58 mission.

Finally, the calibrated accelerations are converted into accelerations along the Orbiter body coordinates by applying the following simple transformation:

$$\begin{pmatrix} X_b \\ Y_b \\ Z_b \end{pmatrix} = \begin{pmatrix} 1 & 0 & 0 \\ 0 & 1 & 0 \\ 0 & 0 & 1 \end{pmatrix} \begin{pmatrix} +X \\ +Z \\ -Y \end{pmatrix} \quad .$$

Model Corrections

The calibrated low-frequency OARE accelerations contain signals other than aerodynamic, such as rotational effects due to the sensor not on the center-of-gravity, and gravity-gradient effects, both in-plane and out-of-plane. Models are applied in order to remove these effects from the acceleration measurements. The application of the models require certain ancillary information that is obtained from NASA-Johnson Flight Center in the form of MSID's. Specifically, the parameters required for any given time are: position, body quaternions(i.e. body orientation), velocity, and p, q, and r - rotation rates about the Shuttle's X, Y, and Z body axes. With these data, gravity-gradient, out-of-plane, and rotational acceleration components are calculated for each body axis from the Orbiter center-of-gravity to the location of the OARE sensor. Each of these components for the three body axes is shown in Figs. 6, 7, and 8. Note that the magnitude of the rotational component is significantly larger than the other two. The total correction to each axis is given in Fig. 9.

Typically, the MSID data are not synchronized to the OARE measurements, thus requiring interpolation. Each of the model accelerations are interpolated to the times of each measured OARE acceleration point.

These interpolated accelerations are then subtracted from the measured data and yield the net accelerations in body coordinates at the Orbiter center-of-gravity, which are, theoretically, the desired aerodynamic accelerations in the absence of noise, thrustor activity, and other extraneous accelerations.

Further Adjustments

The residual acceleration found at the Orbiter center-of-gravity would be solely due to aerodynamic forces on the Orbiter if the correction models and the measurement inputs were perfect, the biases and scale-factor ratios were exact, and there were no other external forces on the Orbiter. Of course, this is not the case and the data must undergo some adjustments in order to extract the aerodynamic accelerations. The first step in this part of the data analysis is to remove obvious large excursions in the acceleration caused by thrustor forces. After these are removed, the following additional effects must be taken into account.

First APU Effect

Significant forces on the Orbiter are generated on a continuing basis by the Orbiter's APUs (Auxiliary Power Units), and must be removed. These 3 units produce pulses of gas which rotate turbines and are used to provide necessary power to move the control surfaces during reentry. The APU gases are ejected from ports at the base of the vertical tail and induce accelerations mainly in the z-body direction. In flight, one of these units is activated prior to deorbit burn. The other two are activated nearly simultaneously after deorbit burn and prior to the entry attitude orientation of 40 degs. It was found that their effect on the X_b-axis is insignificant, but is considerable for the Z_b-axis and smaller, but still significant for the Y_b-axis.

The Z_b-axis data with thrustor activity about the point when the first APU is initiated can be seen in Fig. 10. The adjustments made for the first APU initiation upon the Z_b-and Y_b-axes accelerations can be seen in Figures 11 and 12. Averages of the accelerations before and after APU initiation are performed and the difference taken. The adjustments are 13.382 μg for the Z_b-axis and 2.953 μg for the Y_b-axis. These adjustment values are subtracted from the data set after the initiation of the first APU. The resulting acceleration for all axes is shown in Fig. 13.

First Adjustment

During the Orbiter reentry stage, which begins several hours before deorbit burn, the Orbiter has more thrustor activity in preparation for reentry (as opposed to the orbital phase of the mission) and the payload bay doors are closed which necessitates a more active flash evaporator system (FES). These additional small forces generated by the Orbiter are not modeled, and, in addition, the removal of the first APU effect is not perfect, thus, resulting in a residual acceleration offset. These small adjustments (or zero offsets) can be found for any given axis when the aerodynamic forces are theoretically zero.

Such is the case for the X_b body axis when the angle-of-attack, α is 90 degs. Likewise, the aerodynamic forces in the Z_b-direction disappears when α is 0 or 180 degrees. The aerodynamic forces disappear in the Y_b-direction when β=0 degrees. These adjustments are made by effecting an average of the data near these specific points (i.e. finding a smooth curve which passes through the data on both sides of the point under investigation), and then subtracting this average from the entire data set for the given axis.

The mission time at which α=180 degs. and β=0 degs. occurs is after the initiation of the first APU, at around 334.380 h MET. Adjustments to the Z_b- and Y_b-axes are made as shown in Figs. 14 and 15. The respective adjustments to produce zero accelerations at this time are -3.017 μg and -6.203 μg. The resulting accelerations, after adjustments along all three axes up this point are shown in Fig. 16.

Second & Third APU Effect

Adjustments are also required when the additional two APU's are activated. These are given in Figures 17 and 18 for the Z_b- and Y_b-axes respectively. These adjustments are found to be 19.006 μg for the Z_b-axis and 6.068 μg for the Y_b-axis. The combined effect of the first APU and of APU-2 and -3 are subtracted from the data subsequent to approximately 334.54 h MET.

Further Offset Checks

Removing the effect of the APU's from the data requires an averaging process. In general, experience with averaging techniques has been reliable on past missions, but for this flight the actual turn-on of the remaining APU's were done while the OARE was performing sensor bias calibrations(see Fig. 17). This introduced more error in the process since the data which represented the signal prior to the second and third APU turn-on is more remote (in time) than in past missions. Thus, it is not likely that the second and third APU effect have been completely removed from the data. However, one additional check can be performed on the Z_b-axis data, after all three APU's have been activated, at MET = 334.575 hours. At this time, α = 0, and therefore the residual acceleration along the Z_b-axis at the Orbiter center-of-gravity should be zero. This is illustrated in Figure 19 which calculates the residual acceleration to be 2.08 μg. This is subtracted from the subsequent Z_b-axis data.

Reentry Measurements

The residual accelerations in the X_b- and Z_b-directions in the C range are shown in Figure 20. Each of these accelerations are represented by a 50 point moving average, the ratio A_Z/A_X calculated, and then compared with the free-molecule-flow prediction of C_N/C_A as seen in Fig. 21. Obvious departure from the theoretical prediction are present at lower altitudes as the vehicle transitions from free-molecule-flow to the hypersonic continuum. The departure of A_z/A_x from free-molecule-flow predictions is readily apparent at about 334.68 h MET, at which point the altitude is about 165 km. The corresponding Orbiter orientation, α, is also shown in the upper graph on Fig.

21. These are the first acceleration measurements which clearly show the initial departure from the free-molecule flow regime.

At the very high altitudes, over about 230 km., when the vehicle is at large negative angle-of-attacks, the comparison with the predictions seem to depart as the angle becomes more negative from about 25 degs. The difference appears to be real even though the measurements contain a lot of noise. This departure may be due in part to the gases being injected into the forward flow-field by both the APU's and the FES (the FES predominately expels water vapor over the rear top wing area). As the vehicle pulls its nose up into the flow, and the density increases, as altitude decreases, the effect disappears and the measurements match the predictions quite well.

The accelerations are extended to lower altitudes by including the two other OARE ranges, namely the B and A range data. In these cases for the Z_b-axis, only the effects of the 3 APU's are subtracted. Figure 22 illustrates A_x and A_z for the B and A ranges which corresponds to a lower altitude of approximately 108 km. The ratio, A_z/A_x ,is calculated and compared to the theoretical values of C_N/C_A. This comparison, given on Fig. 23, shows a dramatic departure from theoretical at low altitudes, as expected.

The OARE results extend the earlier measurements by the HiRAP, which has flown over 15 flights on the Challenger and Columbia Vehicles[6,7,8]. HiRAP, unlike OARE, is a gas damped pendulous accelerometer which cannot be calibrated on orbit, and has a resolution of about 1 μg. Because of these limitations, the HiRAP measurements do not reliably extend beyond about 140 km. Thus, the OARE measurements presented in this paper extended the measurements beyond the HiRAP capabilities.

Summary

OARE reentry date has been successfully recorded for the first time during the STS-62 mission from orbital altitudes down to approximately 100 km. This data set has been reduced using biases and scale-factor ratios which were recorded during the orbital part of this mission and information on position, body orientation, velocity, and rotation used to transform accelerations to the Orbiter's center-of-gravity. The effects of APU's have been removed from the data and acceleration components have been checked for offsets when their aerodynamic accelerations should be zero. Ratios of measured aerodynamic accelerations (A_Z/A_X) have been found throughout the entire upper-altitude reentry phase and compared to the theoretical values of C_N/C_A in free molecular flow. As a result, meaningful aerodynamic accelerations have been calculated at much higher altitudes during reentry than previously obtained via HiRAP flights.

The departure from free-molecule-flow to transition into the hypersonic continuum regime is observed in the OARE reentry data and takes place at about 165 km. In addition, in the free-molecule-flow regime, while the vehicle is at negative angles-of-attack during reentry, the free-molecule-flow predictions do not match the measurements. This mismatch appears to correlate with angle-of-attack and altitude. It is surmised that a part of this

prediction mismatch appears to be a result of gases emanating from the Orbiter into the forward flow-field. More detailed investigations are, however, required to resolve this issue.

The OARE aerodynamic ratio data provided in this report represents a milestone in direct measurement of free-molecule flow measurements of a winged orbiting reentry vehicle as it transitions into the hypersonic continuum. Ultimately, this should provide enhanced understanding of the initial transition into the hypersonic continuum by providing a comparison standard for code development, with direct benefits to future space transportation system development.

References

[1]Blanchard, R.C., Hendrix, M.K., Fox, J.C., Thomas, D.J., and Nicholson, J.Y., "The Orbital Acceleration Research Experiment," Journal of Spacecraft and Rockets, vol. 24, no. 6, Nov.-Dec. 1987, pp. 504-511.

[2]Blanchard, R.C., Nicholson, J.Y., Ritter, J.R. and, Larman, K. T. "OARE Flight Maneuvers and Calibration Measurements on STS-58," NASA TM-109093, Apr. 1994.

[3]"Operational Aerodynamic Design Data Book," Rockwell International, Space Division, Downy, CA STS 85-0118 CHG 3, September 1991.

[4]Anon., "Orbital Acceleration Research Experiment Flight Software Requirements," Drawing No. 301018, Rev I, Canopus Systems, Inc., Ann Arbor, MI, Apr., 1988.

[5]Blanchard, R.C., and Nicholson, J.Y., "Summary of OARE Flight Calibration Measurements," NASA TM-109159, Jan. 1995.

[6]Blanchard, R.C.; and Rutherford, J.F.: The Shuttle Orbiter High Resolution Accelerometer Package Experiment: Preliminary Flight Results. Journal of Spacecraft and Rockets, vol. 22, no. 4 July-August 1985, p 474.

[7]Blanchard, R. C.; Larmen, K. T.; and Barrett, M.: The High Resolution Accelerometer Package (HiRAP) Flight Experiment Summary for the First Ten Flights, NASA RP-1267, March 1992.

[8]Blanchard, R. C., Larman, K. T., and Moats C. D., "Flight Calibration Assessment of HiRAP Accelerometer Data," AIAA Paper 93-0836, January 1993.

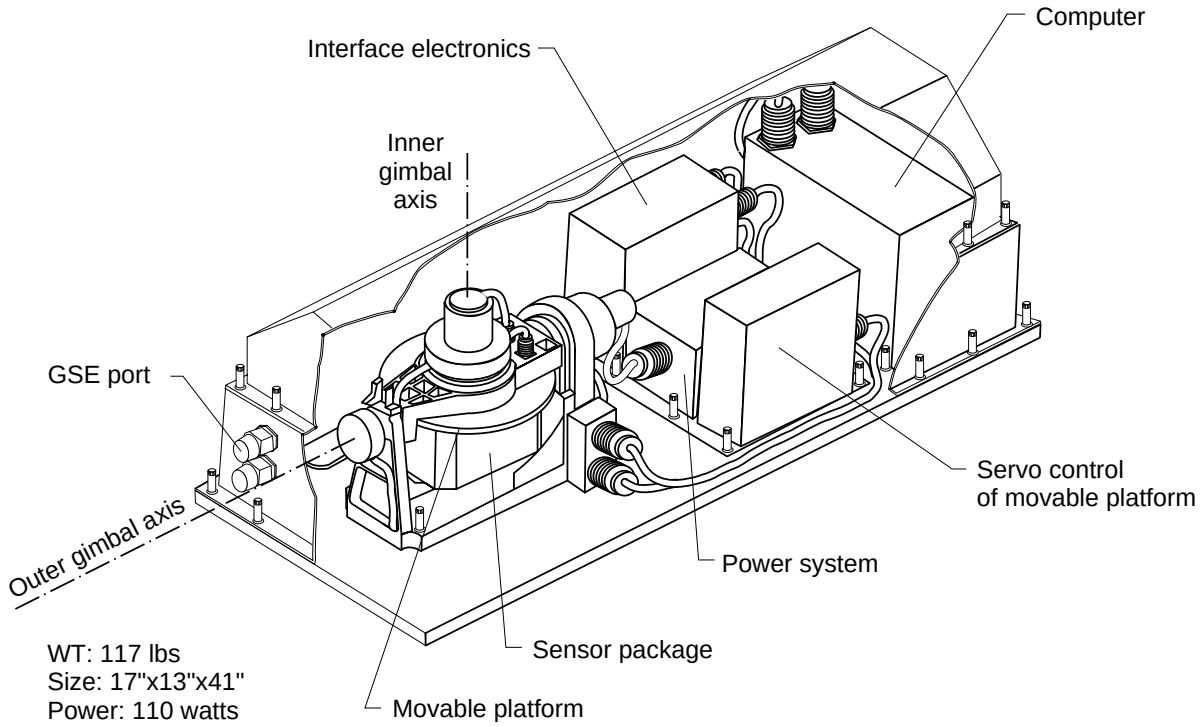

Fig. 1 OARE system layout.

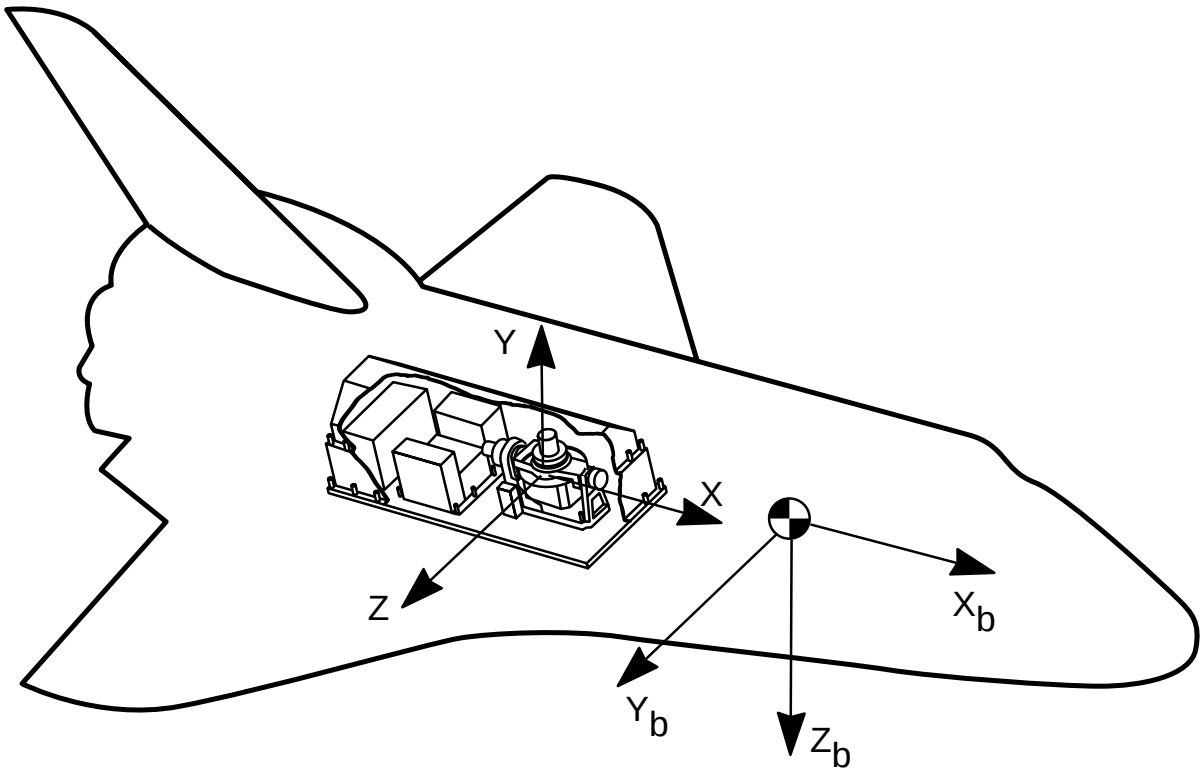

Fig. 2 OARE (X, Y, Z) and Orbiter body axes (X_b, Y_b, Z_b) coordinate systems.

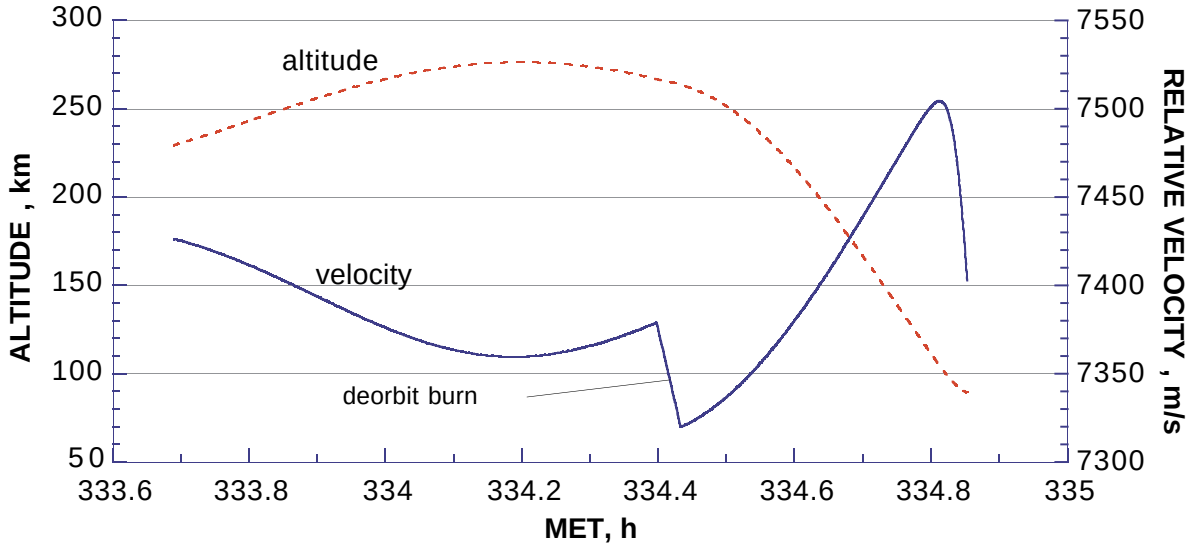

Fig. 3 Altitude and velocity profiles for STS-62.

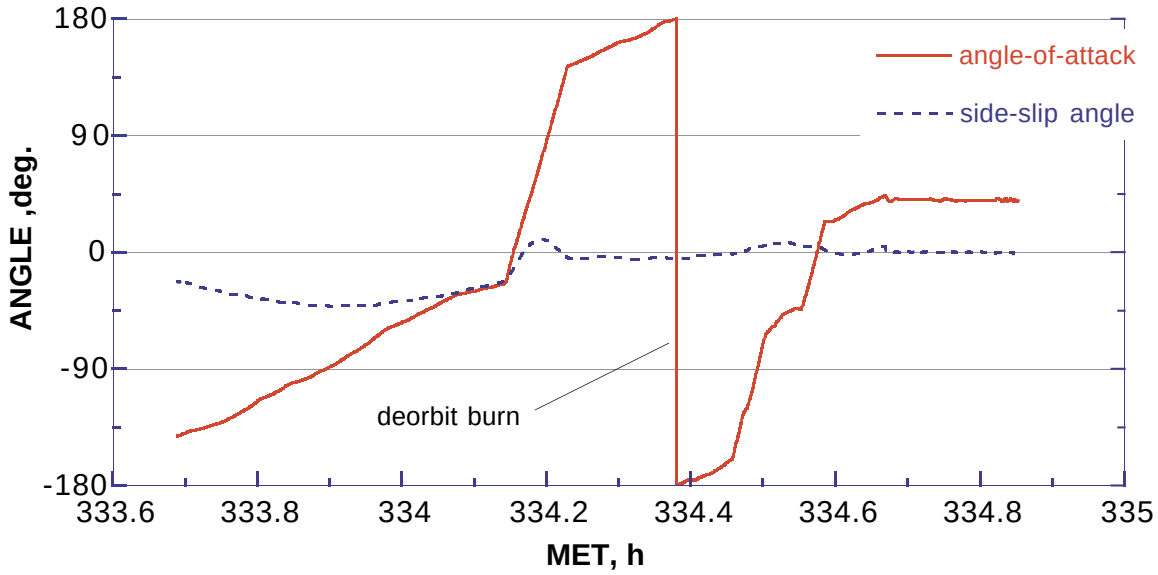

Fig. 4 Angle-of-attack and side-slip angle profiles for STS-62.

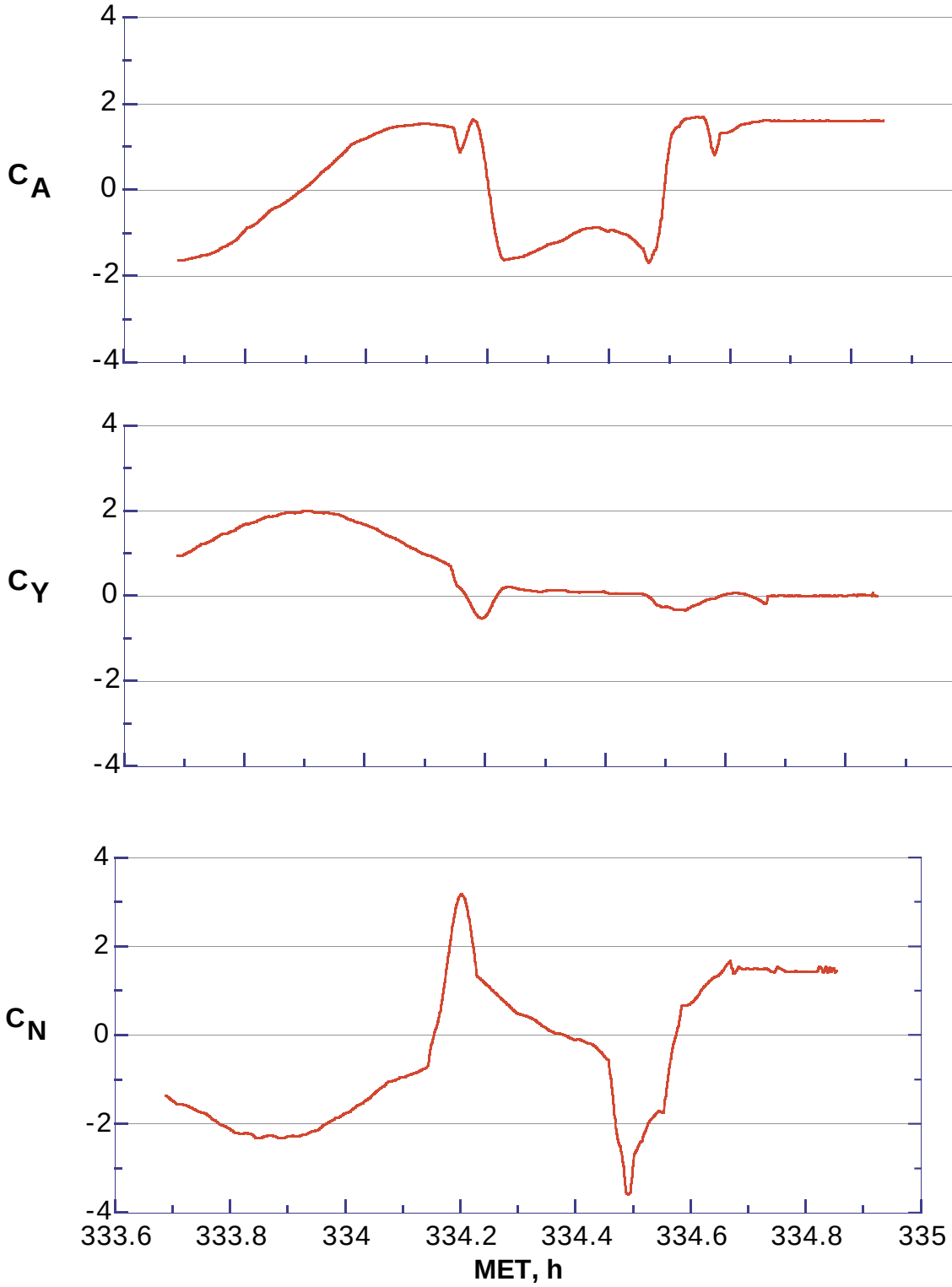

Fig. 5 Predicted free-molecule-flow body axis aerodynamic coefficients for STS-62.

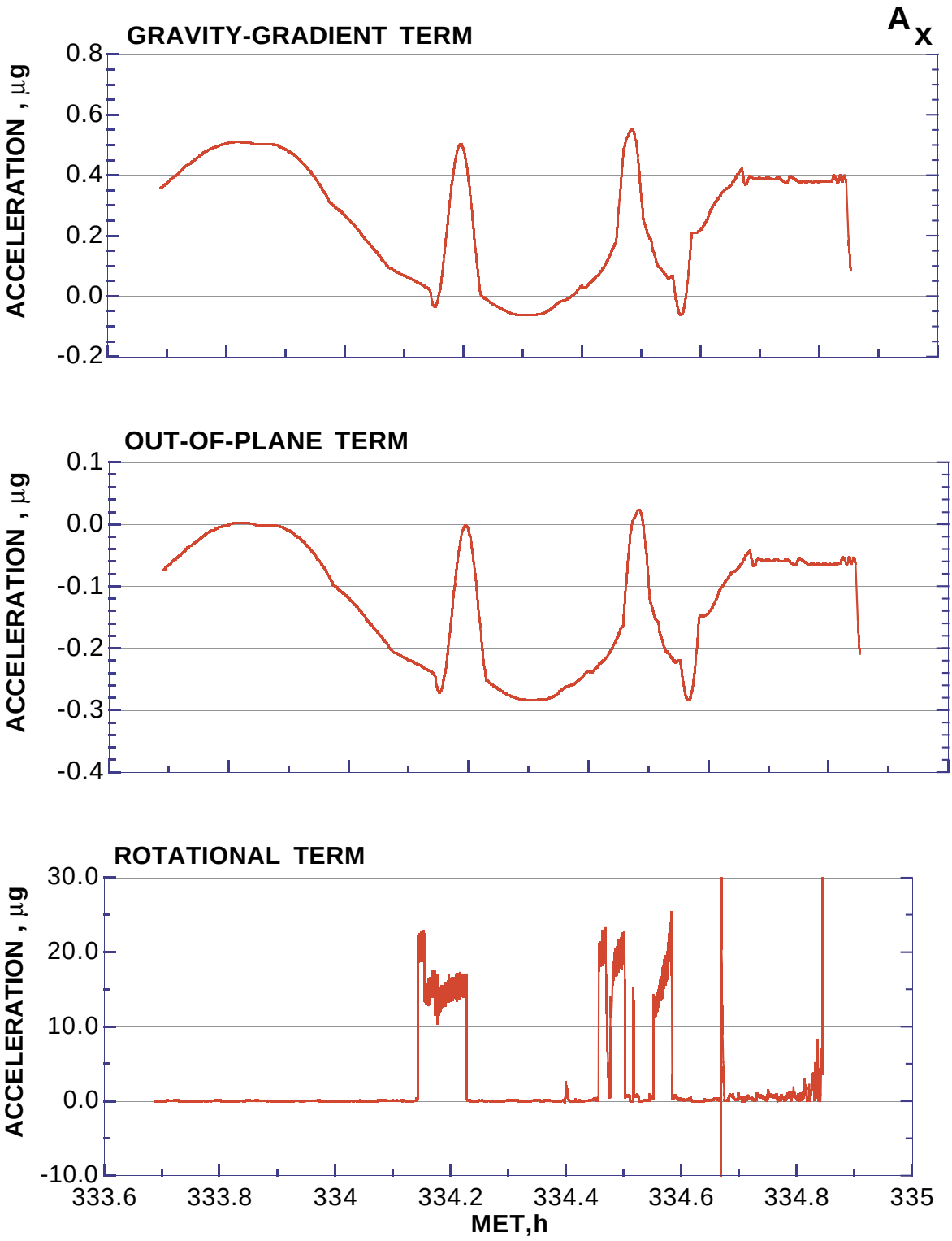

Fig. 6 A_x measurement correction terms for STS-62.

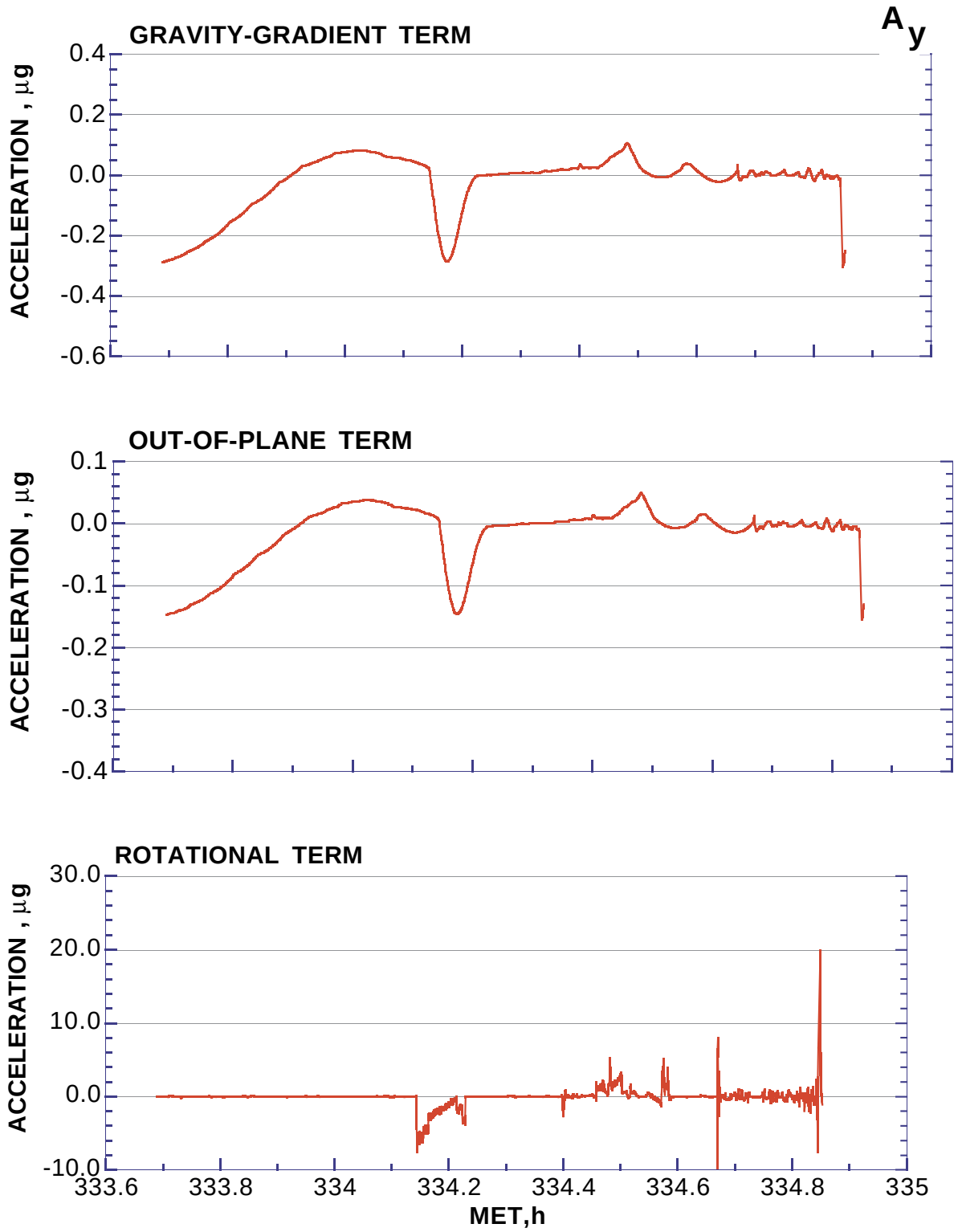

Fig. 7 A_y measurement correction terms for STS-62.

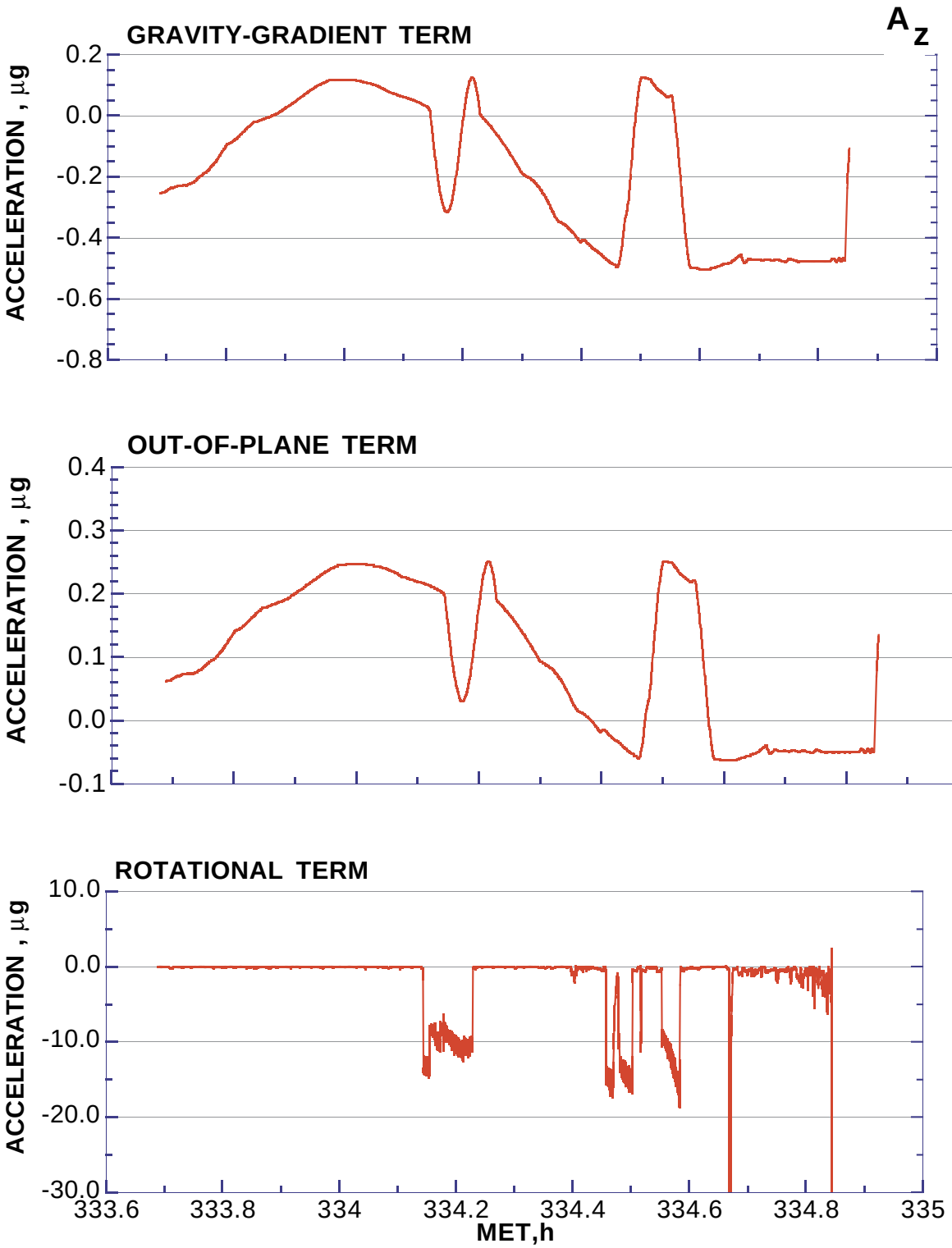

Fig. 8 A_z measurement correction terms for STS-62.

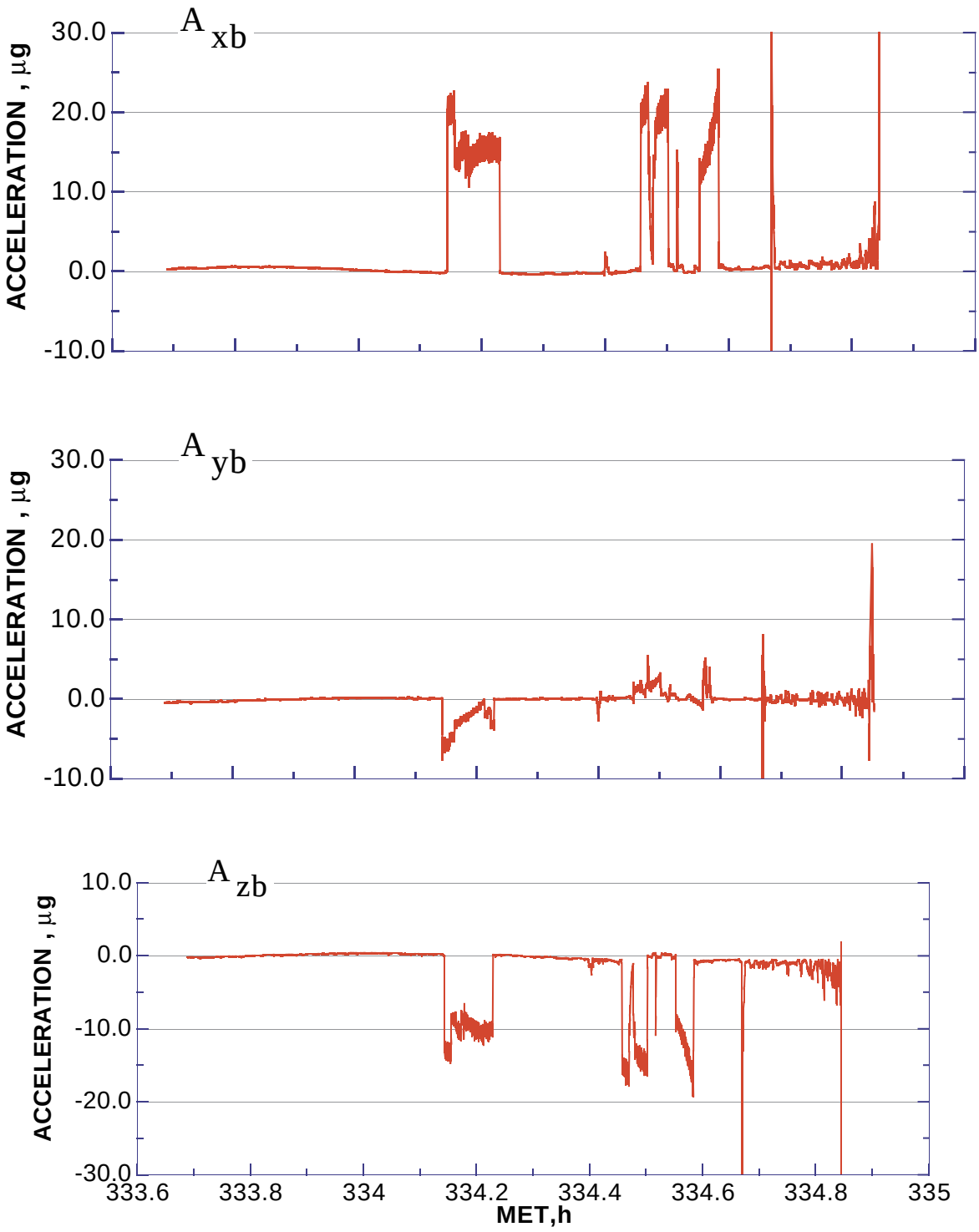

Fig. 9 Total measurement corrections on each axis for STS-62.

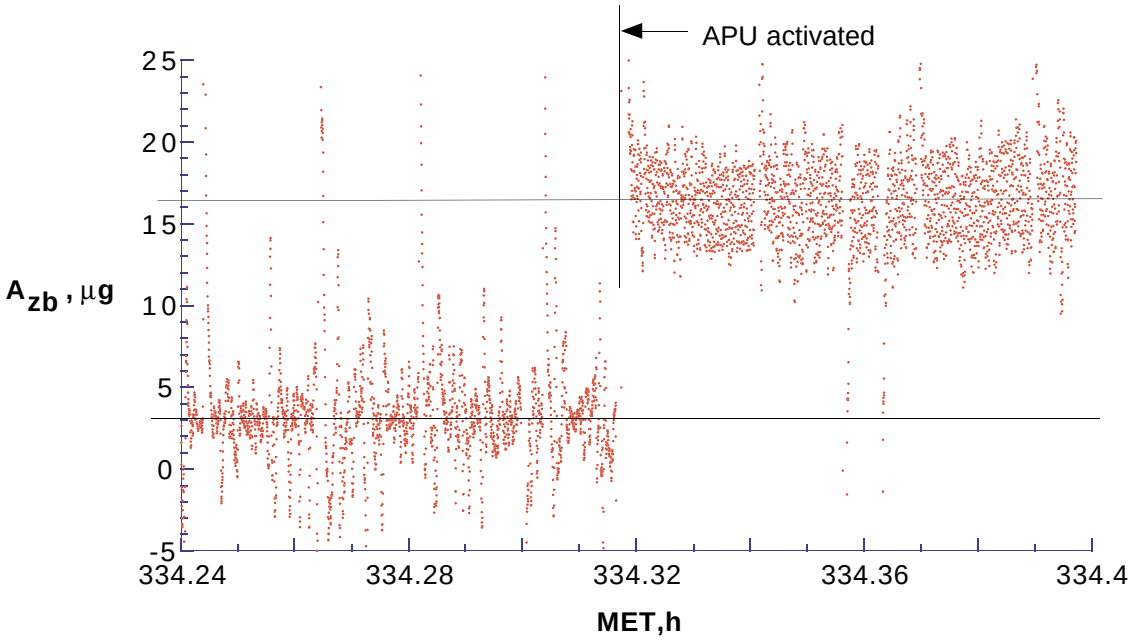

Fig. 10 The effect on A_{zb} due to one APU during STS-62.

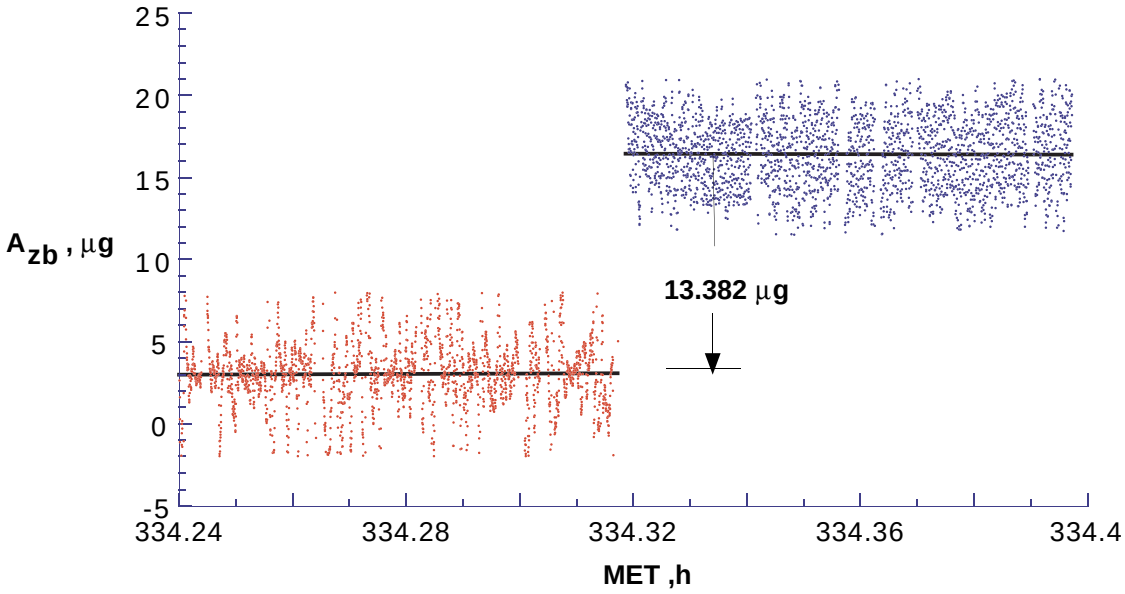

Fig. 11 Data set used to estimate the correction in A_{zb} due to one APU on STS-62.

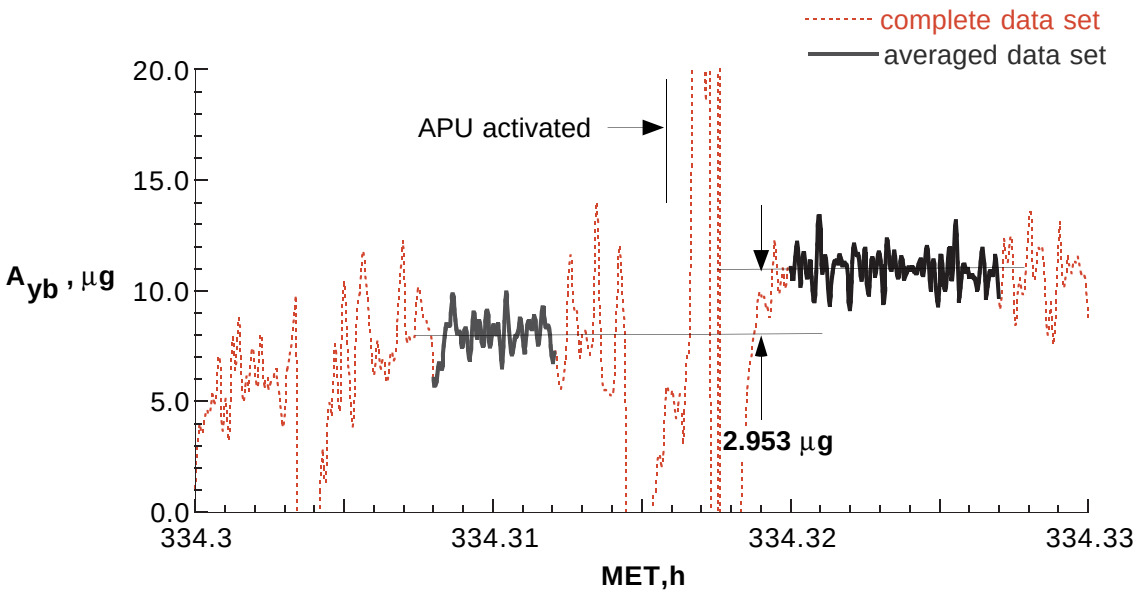

Fig. 12 The effect of one APU on A_{yb} during STS-62.

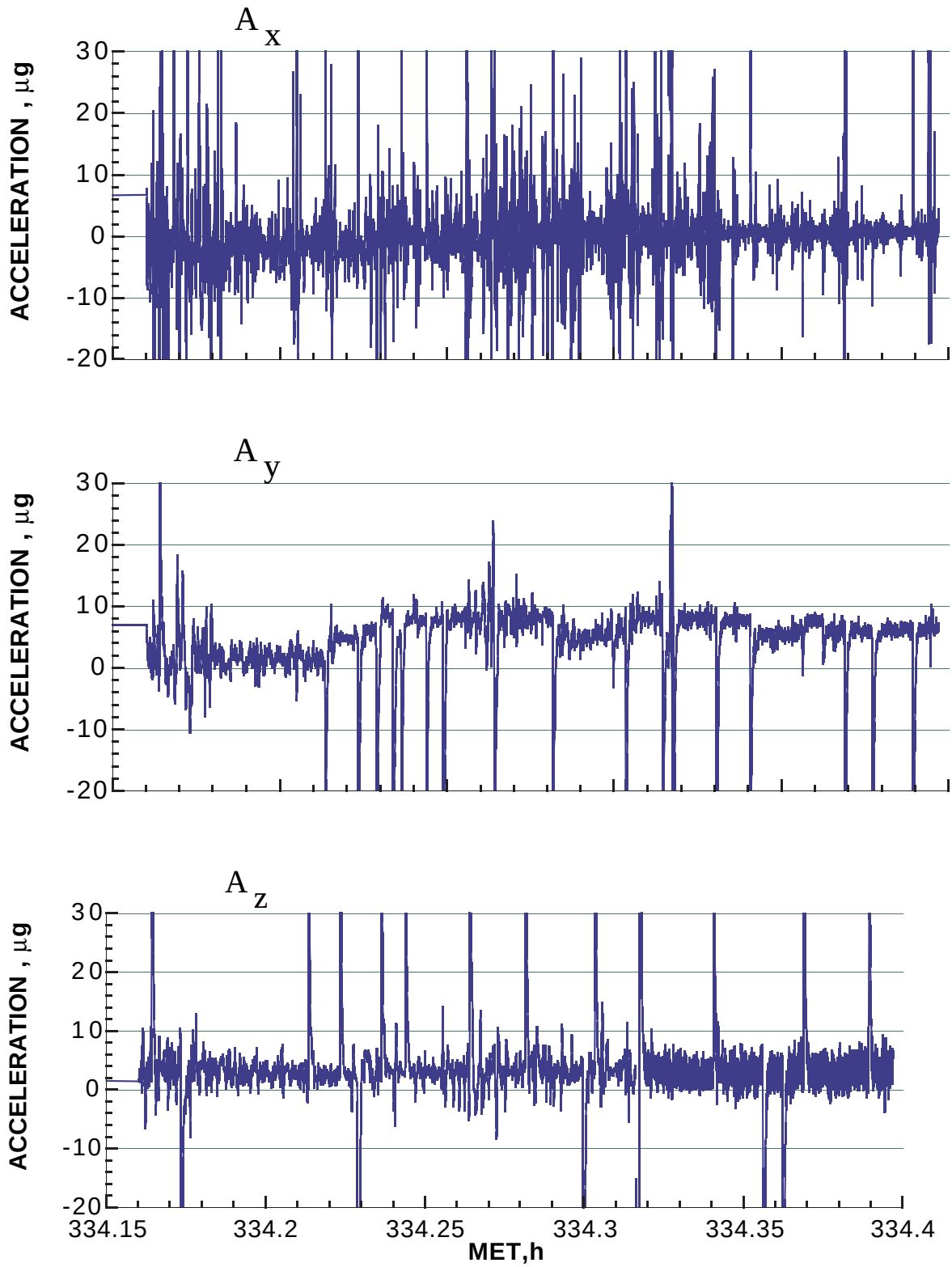

Fig. 13 The body axes accelerations adjusted for 1 APU during STS-62.

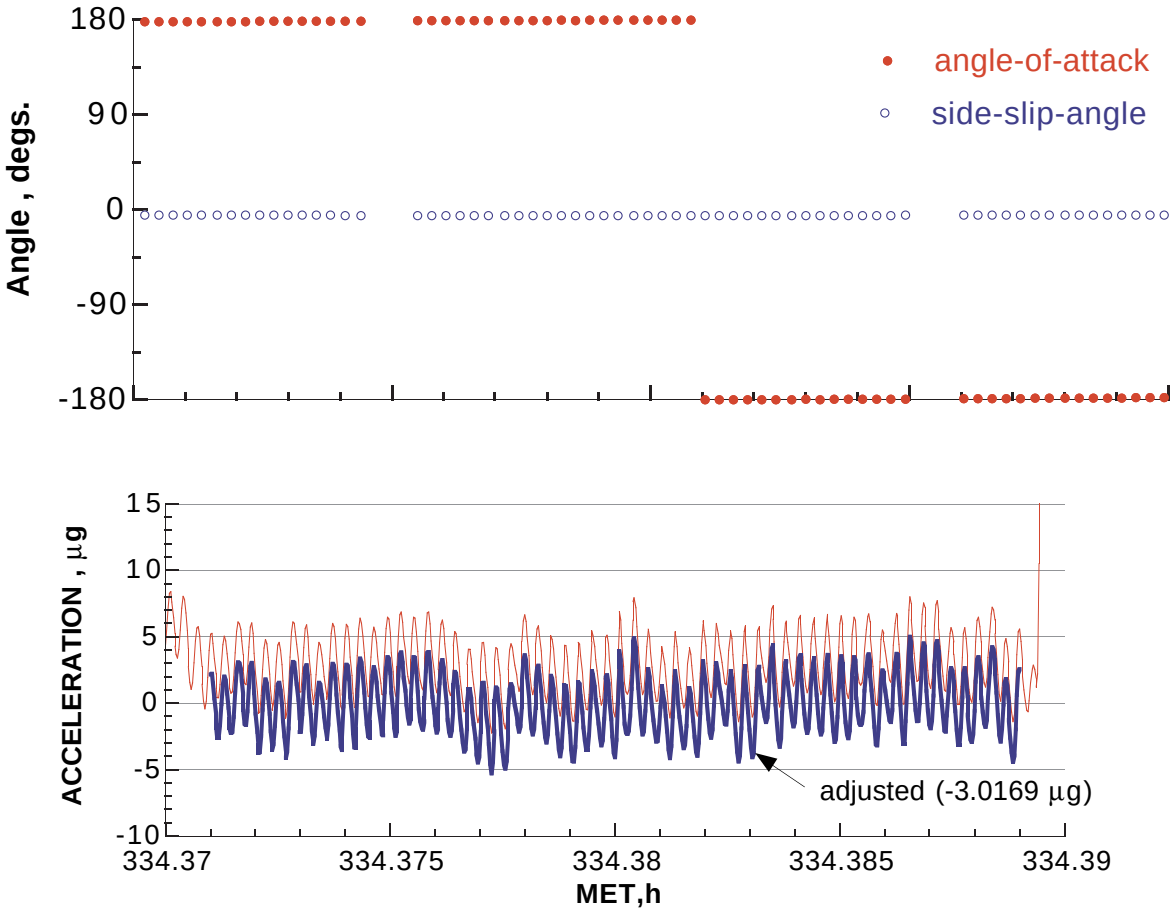

Fig. 14 Adjustment of the A_{zb} center-of-gravity accelerations to zero (C_N=0 @ α=180^o).

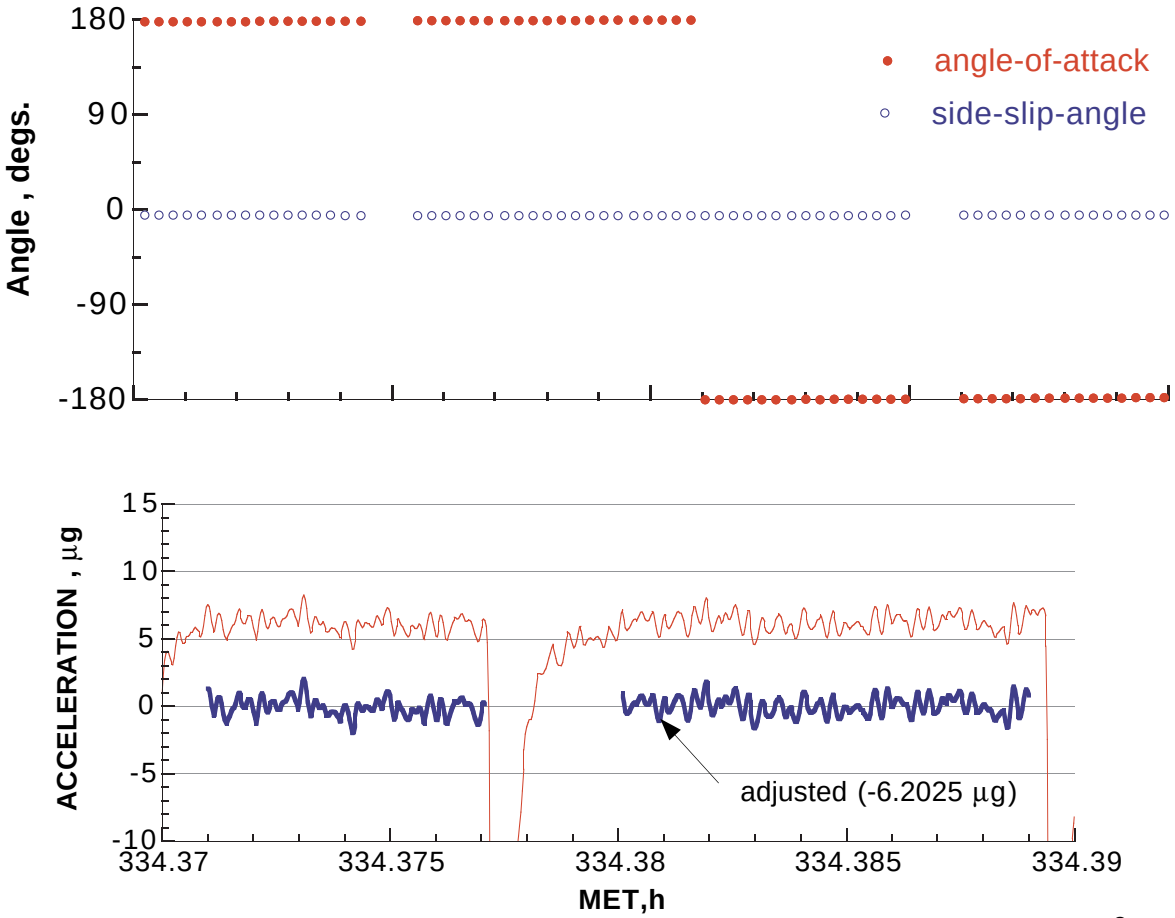

Fig. 15 Adjustment of the A_{yb} center-of-gravity accelerations to zero (C_Y=0 @ β=0^o).

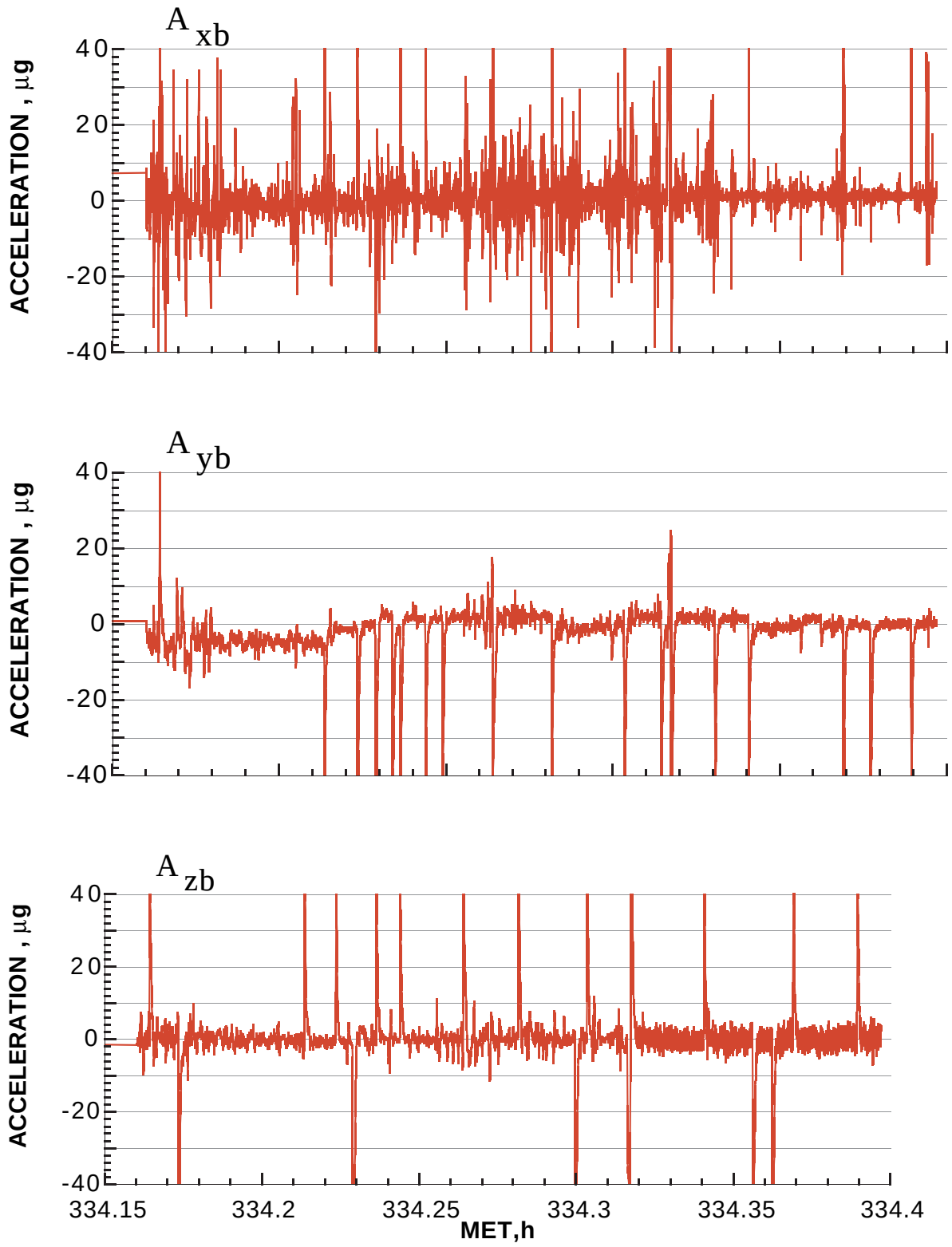

Fig. 16 Body axes accelerations corrected for Orbiter induced offsets.

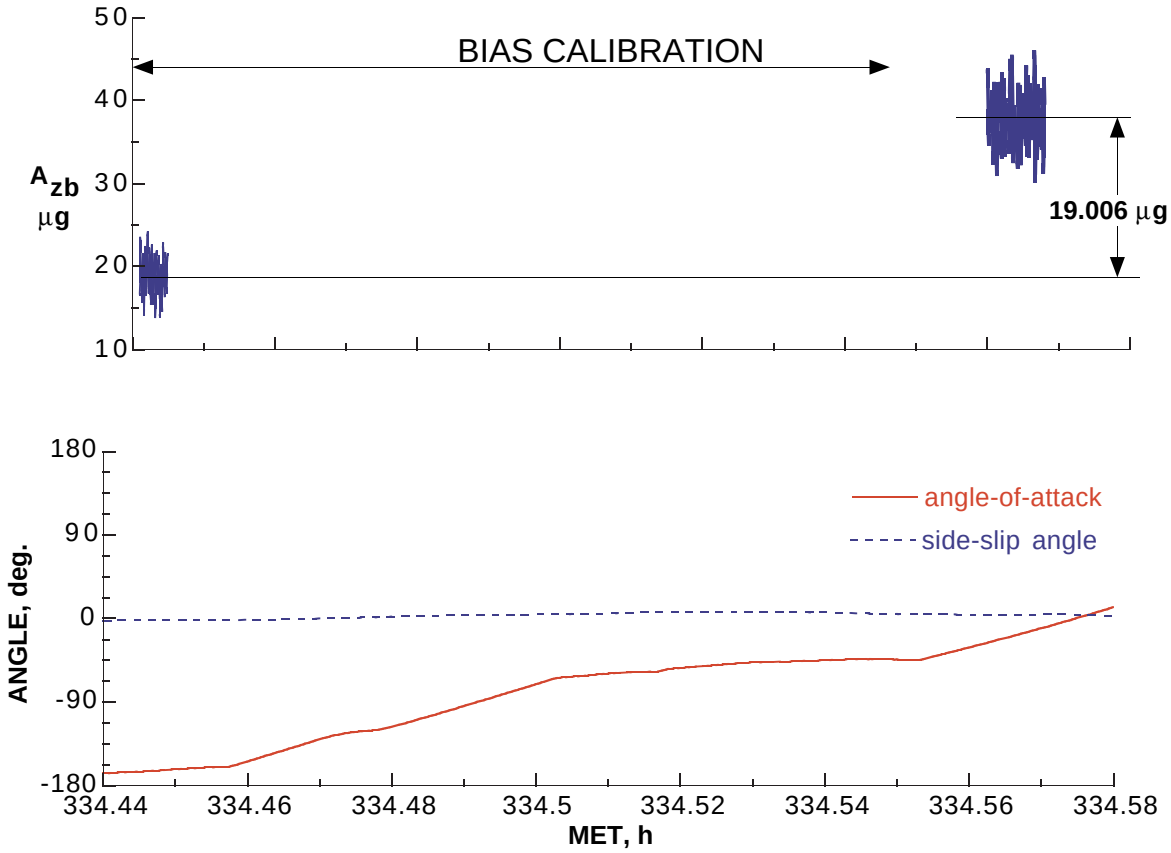

Fig. 17 The effect on A_{zb} due to the second and third APU during STS-62.

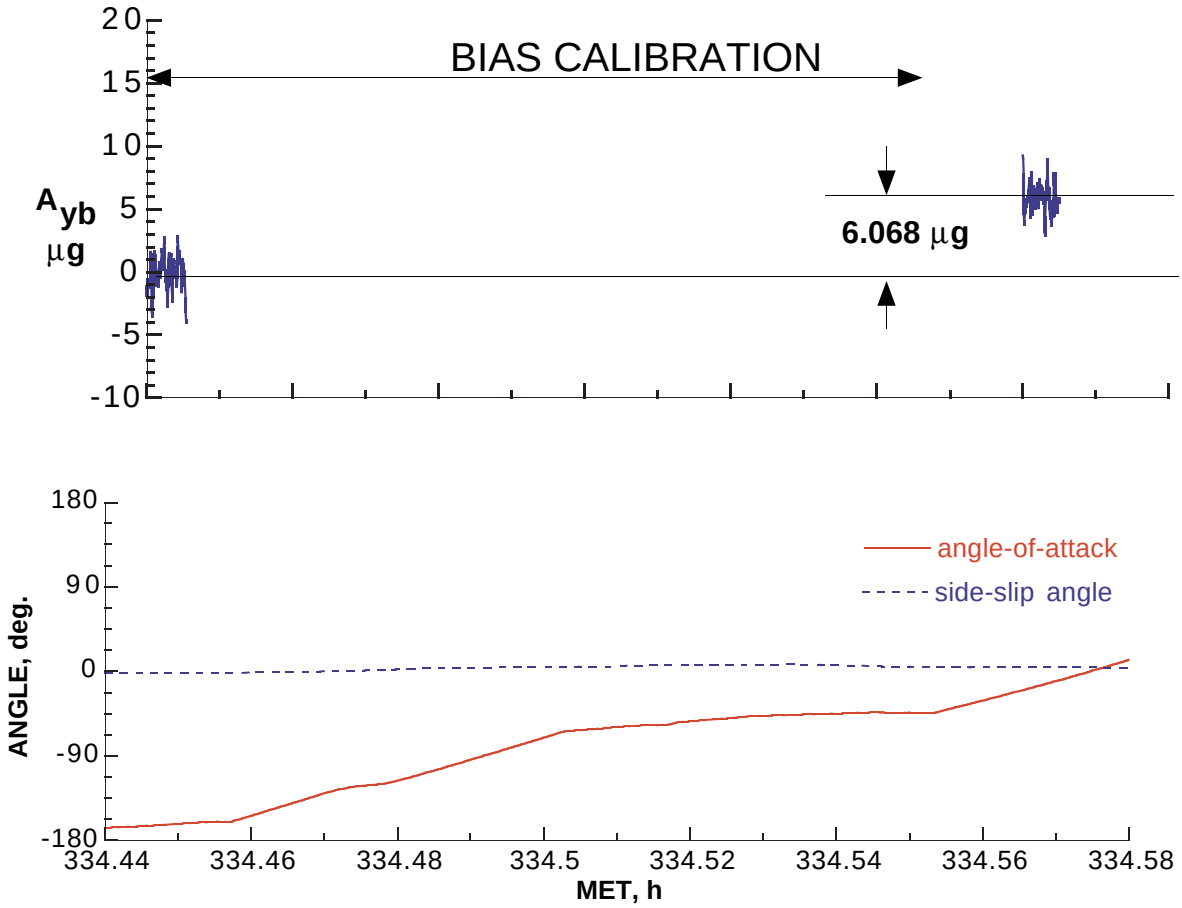

Fig. 18 The effect on A_{yb} due to the second and third APU during STS-62.

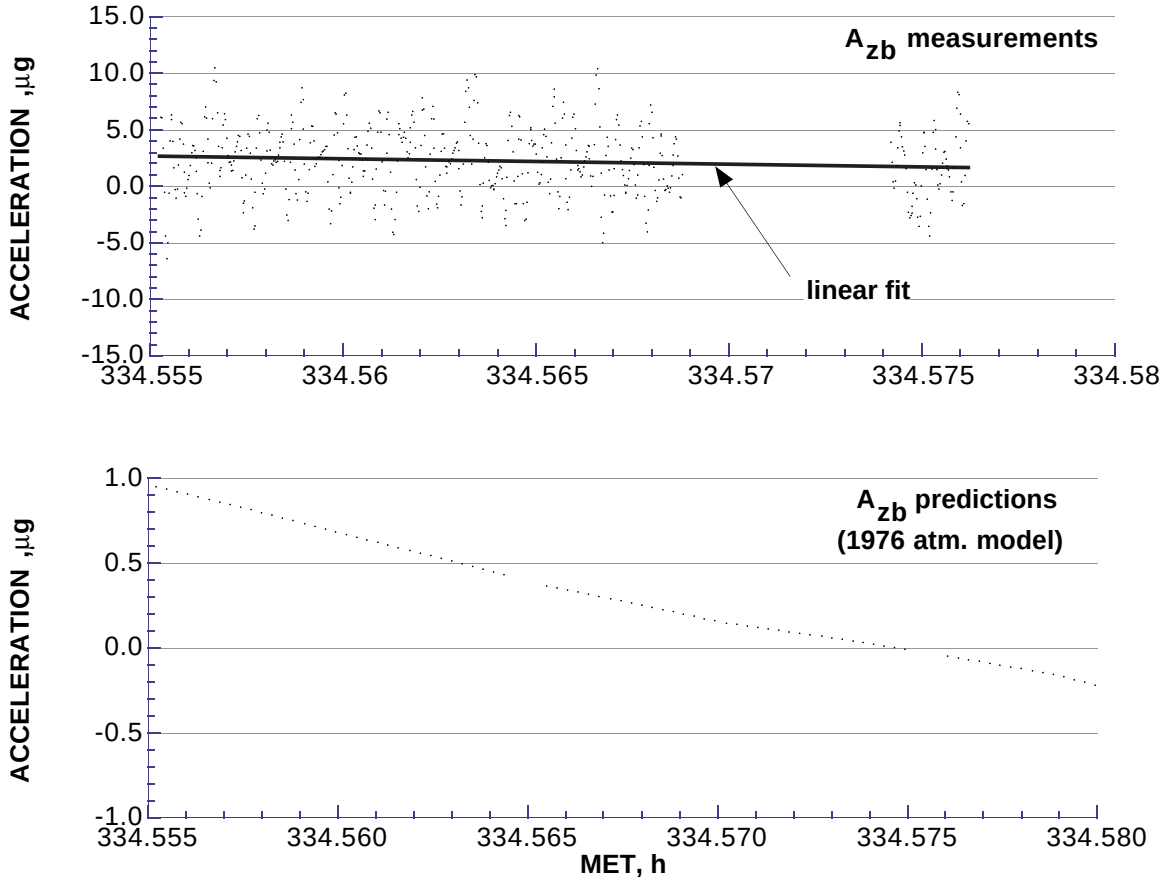

Fig. 19 STS-62 estimate of the residual A_{zb} offset (2.08 μg) based upon predicted zero.

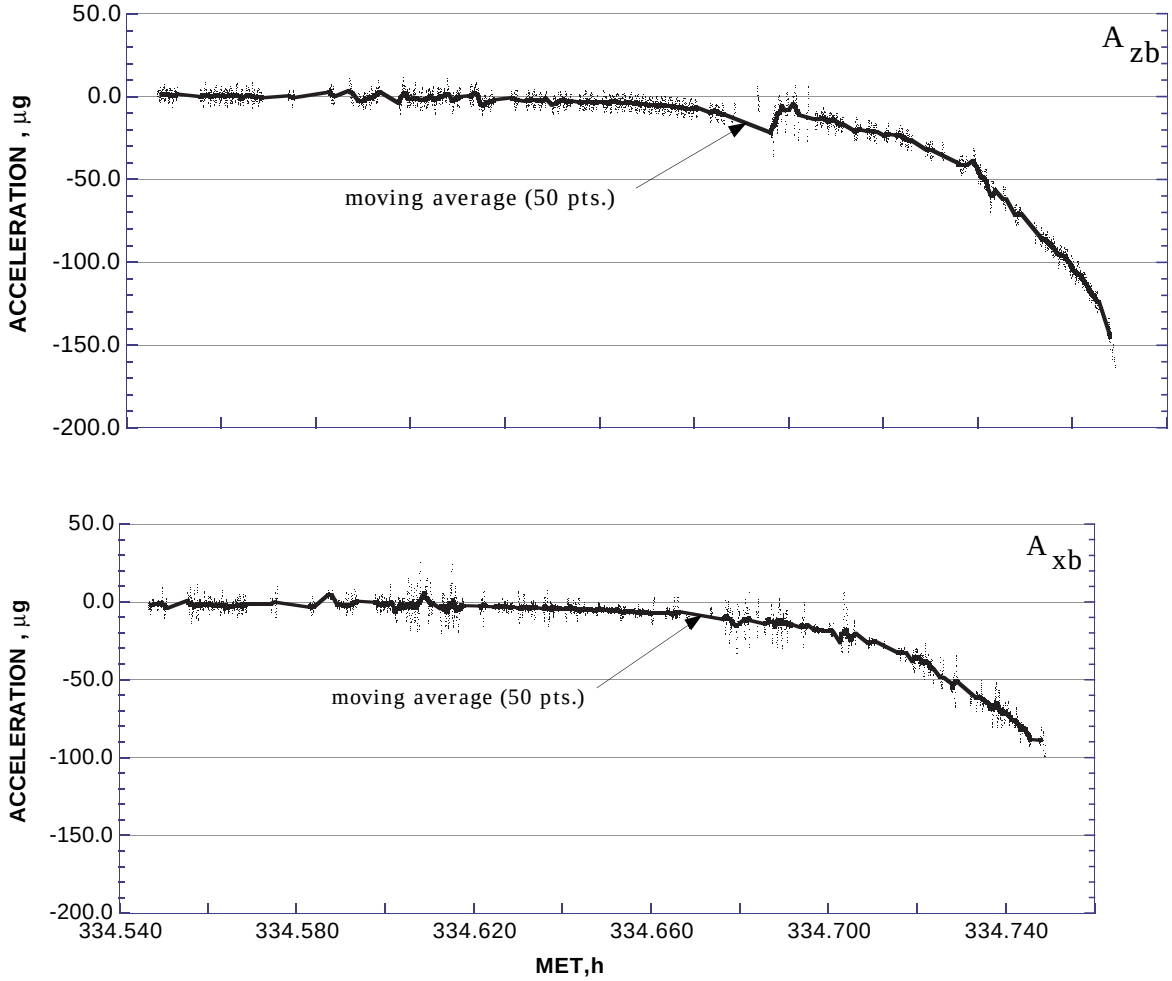

Fig. 20 Normal and axial acceleration measurements at the onset of the free-molecule-flow transition regime.

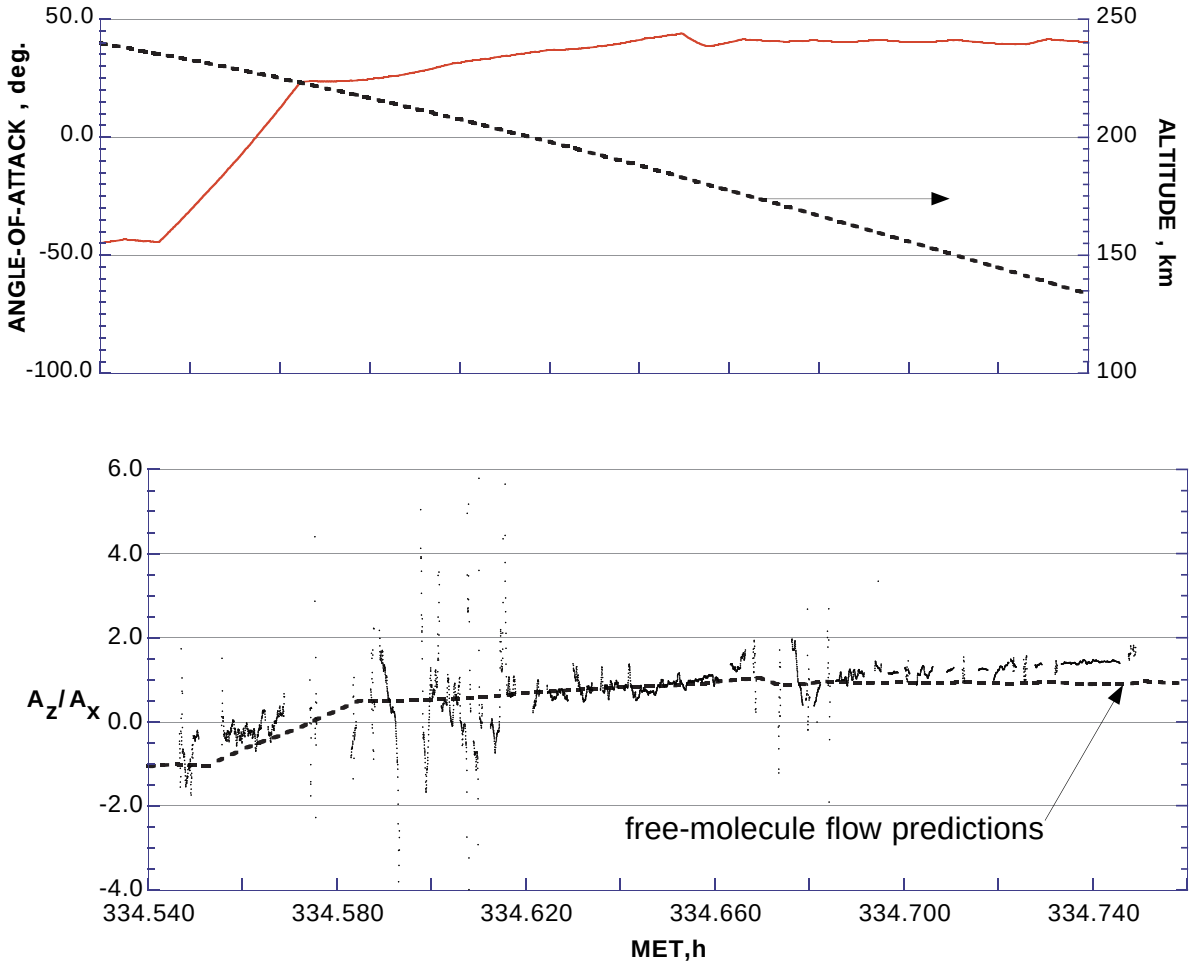

Fig. 21 Normal-to-axial measurements at the onset of rarefied-flow transition regime with corresponding vehicle angle-of-attack and altitiude.

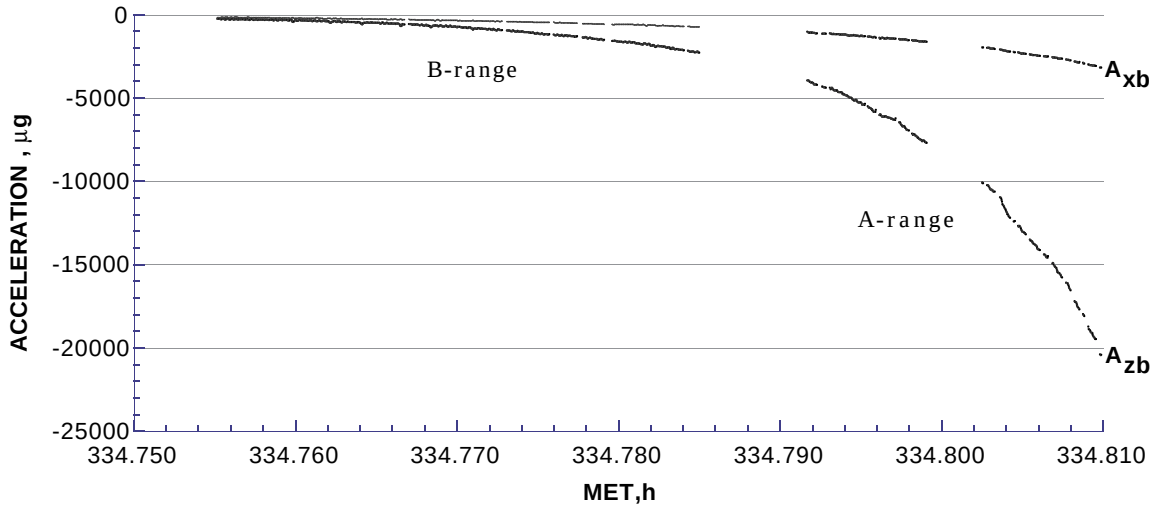

Fig. 22 Normal and axial measurements in the rarefied-flow transition regime.

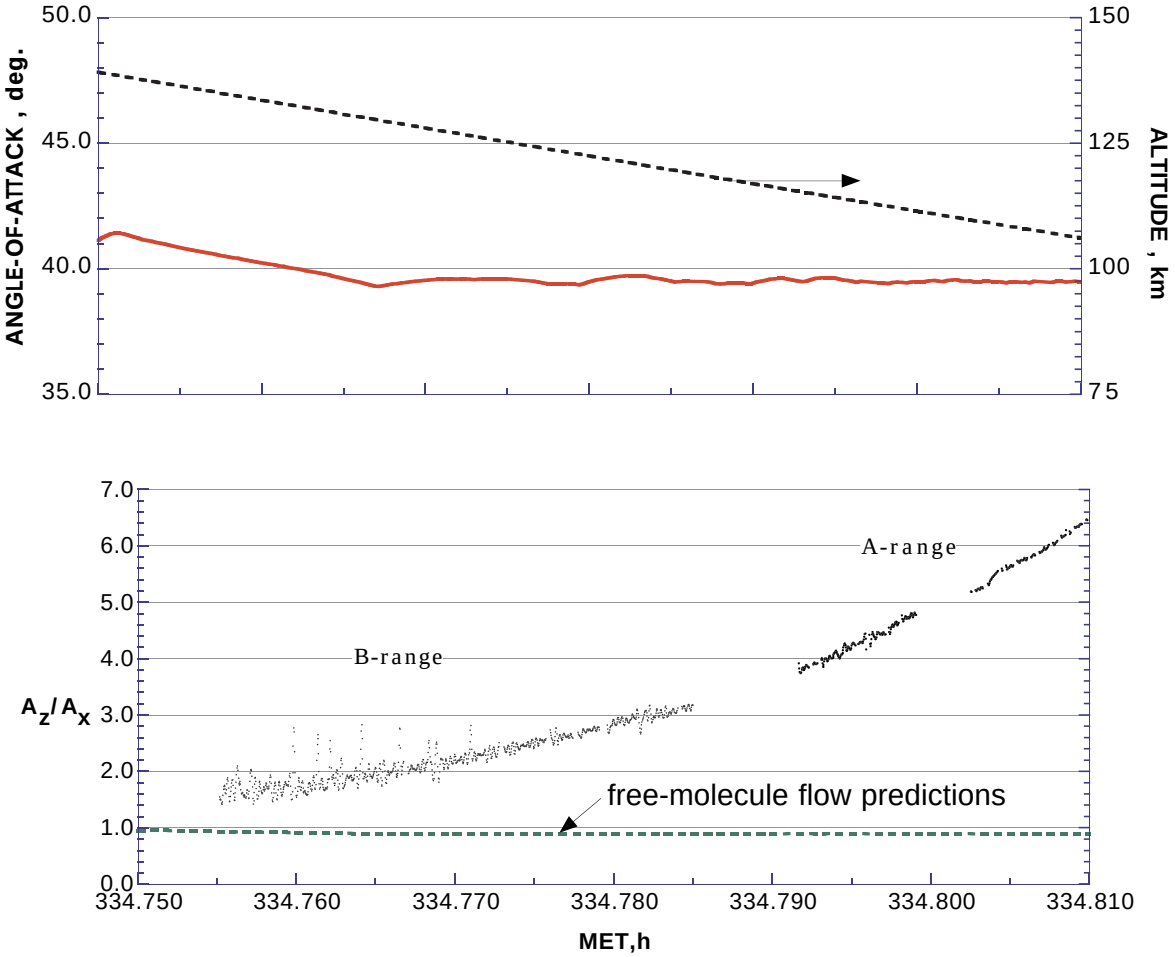

Fig. 23 Normal-to-axial measurements in the rarefied-flow transition regime with corresponding vehicle angle-of-attack and altitiude.